Monomer Exchange and Concentration Fluctuations in Poly(ethylene glycol) Monoalkyl Ether/Water Mixtures. Dependence upon Nonionic Surfactant Composition

T. Telgmann and U. Kaatze*

Drittes Physikalisches Institut, Georg-August-Universität, Bürgerstrasse 42-44, D-37073 Göttingen, Germany

Received: November 23, 1999; In Final Form: March 6, 2000

The ultrasonic absorption spectra between 10^5 Hz and 2×10^9 Hz, the sound velocities at different frequencies, and the shear viscosities of aqueous solutions of the following nonionic surfactants have been measured: C_6E_4, C_6E_5, C_7E_3, C_8E_4, C_8E_5, $C_{10}E_4$, and $C_{12}E_5$. Most C_iE_j/water systems have been considered at different temperatures between 12 and 40 °C and/or at different concentrations (0.01 mol/L $\leq c <$ 0.33 mol/L). The results are compared to those for the triethylene glycol monohexyl ether/water (C_6E_3/H_2O) system reported previously. At solute concentrations around the critical micelle concentration the ultrasonic spectra show one relaxation term due to the formation/decay kinetics of oligomeric species. At higher surfactant content much more complicated spectra reveal the simultaneous presence of various processes. All systems are subject to local fluctuations in the micelle concentration which are described by the Bhattacharjee−Ferrell model here. The spectra for the shorter surfactants C_6E_4, C_6E_5, C_7E_3, and C_8E_5, as those for C_6E_3, in addition to the Bhattacharjee−Ferrell contribution exhibit a lower frequency Hill-type relaxation term which is attributed to the monomer exchange process. With the C_8E_4/water and the $C_{10}E_4$/water systems the monomer exchange equilibrium is reflected by two or one relaxation terms with discrete relaxation time, respectively. In the $C_{12}E_5$/water mixture, as a result of the small monomer concentration, contributions from the exchange process are missing in the spectra. The long chain micelle solutions (C_8E_5, $C_{10}E_4$, $C_{12}E_5$) also show contributions from an ultrahigh-frequency relaxation with relaxation time at around 0.25 ns. It is attributed to the chain rotational isomerization. The parameters of the different molecular mechanisms are discussed, particularly in view of the simultaneous action of the monomer exchange and the fluctuations in the micelle concentration. Also evaluated is the background contribution to the ultrasonic spectra, yielding a shear viscosity relaxation in the megahertz frequency range.

1. Introduction

Due to the great variety in the length of their hydrophobic part and in the hydrogen bonding abilities of their hydrophilic part, the series of poly(ethylene glycol)monoalkyl ethers (C_iE_j) offers favorable conditions for the study of solute/solvent interactions with water. A multitude of experimental methods has been applied in the past to elucidate different types of liquid structures and their molecular dynamics of C_iE_j/water mixtures. Much attention has been directed toward poly(ethylene glycol) monoalkyl ethers which form nonionic micelles in water.[1,2] Particularly interesting are those micellar C_iE_j/water systems which additionally exhibit characteristics of critical demixing. Ultrasonic spectra for such C_iE_j/water mixtures, however, did not show contributions from concentration fluctuations.[3−5] This unexpected result is in contradiction to the widely accepted view that aqueous solutions of nonionic surfactants, at their lower critical solution temperature, may separate into a micelle-poor and a micelle-rich phase[6] and that such micellar systems belong to the same universality class as ordinary binary critical liquids of molecularly dispersed nonionic constituents.[7]

Recently we performed a broad-band ultrasonic spectrometry study on aqueous solutions of triethylene glycol monohexyl ether (C_6E_3).[8] The spectra, measured in the frequency range between 100 kHz and 2 GHz as a function of temperature and surfactant concentration, revealed the existence of contributions from fluctuations in concentration, in excess of the contributions due to the exchange of monomers between the micelles and the suspending phase. The resulting ultrasonic relaxational absorption of the systems appeared to be just the linear superposition of both absorption mechanisms. The parameters of the monomer exchange process, however, indicate relations of the micelle kinetics to the fluctuations in the micelle concentration.

The features of the C_6E_3/water mixtures have increased our interest in the interrelations between the mechanisms of monomer exchange and of the critical concentration fluctuations in nonionic surfactant solutions. In order to study the relative importance of these effects in dependence on the hydrophilic/hydrophobic balance of the surfactant molecules, we performed broadband ultrasonic absorption measurements for mixtures of water with the following poly(ethylene glycol) monoalkyl ethers: C_6E_4, C_6E_5, C_7E_3, C_8E_4, C_8E_5, $C_{10}E_4$, and $C_{12}E_5$. The results for these mixtures at different temperatures and surfactant concentrations are discussed and compared to those for the C_6E_3/water reference system.

2. Experimental Section

Ultrasonic Spectrometry. The sonic absorption coefficient $\alpha(\nu)$ of the liquids has been measured as a function of frequency ν between 100 kHz and 2 GHz and also determined has been the sound velocity $c_s(\nu)$ of the samples at some selected frequencies using the same methods as in the C_6E_3/water study.[8] We utilized particularly a plano-concave (100 kHz $\leq \nu \leq$ 2.7 MHz[9]) as well as a biplanar (800 kHz $\leq \nu \leq$ 15 MHz[10]) cavity resonator cell for fixed path length continuous wave measure-

10.1021/jp994159d CCC: $19.00
Published on Web 05/02/2000

TABLE 1: Critical Micelle Mass Fraction Y_{cmc}, Mean Aggregation Number $\bar{m}$ of Micelles, Critical Demixing Temperature T_{crit}, and Mass Fraction Y_{crit} of the Critical Mixture, as well as Amplitude ξ_0 of the Fluctuation Correlation Length (Eq 1) for the C_iE_j/Water Systems[a]

surfactant	Y_{cmc}, 10^{-2}	$\bar{m}$	T_{crit}, °C	Y_{crit}, 10^{-2}	ξ_0, *nm*
C_6E_3	2.0	57	46.0	14.6	0.35
C_6E_4	2.0	56*	66.3	16.4	0.30
C_6E_5	2.3	55	78.4		
C_7E_3	0.6*	80*	22.8	8*	0.45*
C_8E_4	0.20	82	39.8	7.1	0.54
C_8E_5	0.35	80	59.6	9.6	
$C_{10}E_4$	0.027	100	18.2	2.0	1.07
$C_{12}E_5$	0.0039	160	29.6	1.5	1.4

[a] Data from the literature[1,3,5,15−19] and from our measurements (T_{crit}). The asterisk indicates values obtained by interpolation of data of similar systems. In doing so first C_iE_j with identical j and different i have been considered. Afterward the small dependence upon j has been taken into account.

ments and four cells for variable path length pulse-modulated wave transmission measurements (3 MHz ≤ ν ≤ 60 MHz;[11] 3 MHz ≤ ν ≤ 120 MHz;[12] 30 MHz ≤ ν ≤ 500 MHz;[13] 500 MHz ≤ ν ≤ 2 GHz[14]).

The temperature T of the samples was controlled and measured to within 0.02 K. Differences in the temperature of different cells thus did not exceed 0.04 K. The error in the α data depends on the properties of the samples and on the temperature of measurement. It may be globally characterized by $\Delta\alpha/\alpha = 0.05$ at $\nu < 3$ MHz, $\Delta\alpha/\alpha = 0.02$ at 3 MHz ≤ ν ≤ 50 MHz, and $\Delta\alpha/\alpha = 0.01$ at $\nu > 50$ MHz. The error in the sound velocity values is $\Delta c_s/c_s = 0.001$ at $\nu < 3$ MHz and $\nu >$ 500 MHz and it is $\Delta c_s/c_s = 0.0005$ at 3 MHz ≤ ν ≤ 500 MHz. Fluctuations in the frequency were negligibly small.

Nonionic Surfactant Solutions. In Table 1 some parameters are displayed that characterize the micelle formation and critical demixing characteristics of the C_iE_j/water systems under consideration. With the exception of the indicated data the values for the critical micelle mass fraction Y_{cmc}, the mean aggregation number $\bar{m}$ of micelles, the mass fraction Y_{crit} of the critical mixture, and the amplitude ξ_0 of the correlation length

$$\xi(T) = \xi_0 t^{-\tilde{\nu}} \tag{1}$$

have been taken from the literature.[1,3,5,15−19] Here

$$t = (T_{crit} - T)/T_{crit} \tag{2}$$

denotes the reduced temperature and $\tilde{\nu}$ is the critical exponent of the correlation length. Within the framework of the Landau−Wilson−Ginsburg model of critical fluctuations $\tilde{\nu} = 0.63$.[19] For all but the C_6E_4/water system the critical temperature T_{crit} has been determined to within ±0.04, K using the actual mixture of critical composition. For this purpose the He−Ne laser light scattered from the samples has been monitored at slowly rising sample temperature.

Tetraethylene glycol (C_6E_4) and pentaethylene glycol (C_6E_5) monohexyl ether, triethylene glycol monoheptyl ether (C_7E_3), tetraethylene glycol (C_8E_4), and pentaethylene glycol (C_8E_5) monooctyl ether, as well as tetraethylene glycol monodecyl ether ($C_{10}E_4$) have been purchased from Bachem Biochemica (Heidelberg, FRG). Pentaethylene glycol monododecyl ether ($C_{12}E_5$) has been delivered by Fluka (Neu-Ulm, FRG). All compounds, with a purity grade between 97% and 99%, have been used as delivered by the manufacturers. The sample liquids have been prepared by weighing appropriate amounts of the surfactant into suitable flasks which were filled to the line measure with deionized, additionally bidistilled and UV-sterilized water. The density ρ of the samples has been measured pycnometrically. The (static) shear viscosity η_s of the mixtures has been determined using a falling ball viscometer (Haake, Berlin, FRG).

When not used in measurements, the samples were stored in a refrigerator. Care was taken to complete all measurements within a few days after sample preparation. No variations of the critical demixing temperature T_{crit} were observed during the period of measurements.

A survey of the C_iE_j/water mixtures along with their concentration, density, viscosity, and sound velocity data is given in Table 2.

3. Results and Treatment of Ultrasonic Absorption Spectra

General Aspects. In Figure 1 an ultrasonic absorption spectrum of the C_7E_3/water system is presented in the format $(\alpha\lambda)_{exc}$ vs ν. Here $\lambda = c_s/\nu$ is the sonic wavelength and

$$(\alpha\lambda)_{exc} = \alpha\lambda - B\nu \tag{3}$$

is the absorption per wavelength in excess of the asymptotic high-frequency (background) absorption, with coefficient B independent of ν. The excess absorption spectrum displayed in Figure 1 shows a feature that is characteristic of most ultrasonic spectra under consideration. It exhibits $(\alpha\lambda)_{exc}$ contributions over a broad frequency range. The full curve also displayed in the figure is the graph of a sum of four Debye-type relaxation terms, each term given by an expression of the form

$$R_D(\nu) = \frac{A_D \omega \tau_D}{1 + \omega^2 \tau_D^2} \tag{4}$$

In this term A_D is the relaxation amplitude, τ_D is the (discrete) relaxation time, and $\omega = 2\pi\nu$. As illustrated by the spectrum of the C_7E_3/water mixture in Figure 1, a sum of four terms with discrete relaxation time can fairly well account for the measured data. There exist, however, systematic deviations of the measured data from the relaxation spectral function, indicating that the four-Debye-term model does not mean the optimum description of the experimental spectra. In conformity with the treatment of the C_6E_3/water spectra,[8] we thus also apply relaxation spectral terms that are based on a continuous distribution of relaxation times. Particular attention is paid to the restricted Hill term $R_H^{\#}(\nu)$ [8,20] and the Bhattacharjee−Ferrell term $R_{BF}(\nu$.[21,22] The former is defined by

$$R_H^{\#}(\nu) = 2^{1/s_H - 1} A_H^{\#} \frac{\omega\tau_H}{(1 + (\omega\tau_H)^{2s_H})^{1/s_H}} \tag{5}$$

with the amplitude parameter $A_H^{\#}$, a characteristic relaxation time τ_H, and a relaxation time distribution parameter s_H. The $R_H^{\#}(\nu)$ term represents the monomer exchange between the micelles and the suspending phase[8,23] which, according to the extended Teubner−Kahlweit model of micelle kinetics[24] at surfactant concentrations near the critical micelle concentration (cmc), is predicted to deviate from the simple Debye relaxation behavior. The deviations are correlated to the absence of a distinct minimum in the oligomer range of the size distribution of short-chain amphiphile systems near their cmc.[24] The existence of a relaxation time distribution has in parts been explained by a development of the extended Teubner−Kahlweit model of stepwise association in terms of Debye-type contributions. That analysis indicated the simultaneous presence of two

TABLE 2: Mole Fraction *x*, Mass Fraction *Y*, and Molar Concentration *c* of Surfactant, as well as Density ρ, Static Shear Viscosity η_s, and Sound Velocity at two Frequencies for the C_iE_j/Water Mixtures Displayed at the Temperatures *T* of Measurement

							c_s, m/s	
C_iE_j	x, 10^{-2} ±0.2%	Y, 10^{-2} ±0.1%	c, mol/L ±0.2%	T, °C	ρ, g/cm^3 ±0.1%	η_s, 10^{-3} Pa·s ±0.2%	*300 kHz* ±0.1%	100 *MHz* ±0.05%
C_6E_4	0.560	8.0	0.287	17.5	1.002	1.547	1503.7	1509.8
				25.0	1.00	1.267	1514.6	1521.1
				32.5	0.998	1.075	1523.1	1530.3
				40.0	0.995	0.929	1530.3	–
C_6E_5	0.234	4.0	0.125	25.0	0.999	1.046	1518.3	1519.3
	0.350	5.9	0.183	25.0	1.000	1.116	1518.9	1521.6
C_7E_3	0.627	8.0	0.322	12.0	1.001	2.249	1469.8	1473.6
				19.0	0.999	2.078	1485.4	1488.6
				21.0	0.998	2.057	1489.2	1492.5
				22.5	0.998	2.071	1491.7	1498.1
C_8E_4	0.213	3.5	0.114	17.5	0.999	1.308	1481.5	1481.3
				25.0	0.998	1.116	1499.0	1500.7
				32.5	0.995	1.046	1512.6	1514.9
				39.0	0.993	1.020	1522.1	–
	0.447	7.1	0.232	17.5	0.999	1.768	1484.4	1484.4
				25.0	0.998	1.648	1498.9	1501.7
				32.5	0.995	1.633	1510.1	1513.2
				39.0	0.992	1.661	1518.0	–
C_8E_5	0.018	0.37	0.010	25.0	0.997	0.924	1498.9	1498.5
	0.235	4.74	0.125	25.0	0.998	1.100	1502.2	1502.7
	0.345	6.81	0.18	25.0	0.998	1.279	1500.3	1503.9
	0.470	9.07	0.24	25.0	0.998	1.559	1503.3	1503.9
$C_{10}E_4$	0.110	2.0	0.060	12.0	1.000	2.353	1458.7	1460.7
				14.0	1.000	2.384	1465.2	1465.7
				16.0	1.000	2.451	1471.6	1472.2
				18.0	0.999	2.497	1478.1	1478.2
$C_{12}E_5$	0.067	1.5	0.037	17.5	0.999	2.224	1476.7	1479.1
				25.0	0.997	2.896	1496.6	1496.7
				29.4	0.996	3.234	1506.7	1506.9

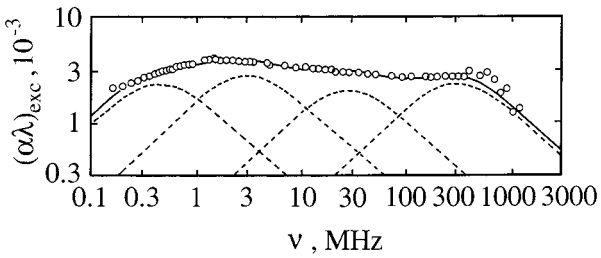

Figure 1. Ultrasonic excess absorption spectrum of the C_7E_3/H_2O mixture with mass fraction $Y = 0.08$ of surfactant at 22.5 °C. Dashed curves are graphs of relaxation terms with discrete relaxation time, respectively. The full curve represents the sum of these terms.

relaxation modes, with similar relaxation rates and comparable amplitudes, in the ultrasonic spectra corresponding with the isodesmic scheme of coupled reactions near the cmc.[24] The particular shape of the relaxation time distribution underlying the restricted Hill term (eq 5) is of low significance here. For this reason $R_H^{\#}$ has been used for convenience, especially because this relaxation term allows for a suitable representation of various experimental spectra of solutions of amphiphiles near their cmc.[8,23]

The $R_{BF}(\nu)$ term represents the Bhattacharjee−Ferrell theory of critical concentration fluctuations.[21,22] It is given by

$$R_{BF}(\nu) = A_{BF}\omega^{-\tilde{\alpha}/(z\tilde{\nu})}F(\Omega) \qquad (6)$$

with the amplitude

$$A_{BF} = \hat{A}_{BF}\frac{\pi\tilde{\alpha}}{2z\tilde{\nu}}\omega_0^{\tilde{\alpha}/(z\tilde{\nu})} \qquad (7)$$

In this relation $\tilde{\alpha}$ denotes the critical exponent for the specific heat and z the dynamical critical exponent, and ω_0 is the amplitude of the angular frequency (relaxation rate) of order parameter fluctuations. The scaling function F in eq (6) is given by

$$F(\Omega) = \frac{3}{\pi}\int_0^\infty \frac{x^3}{(1+x^2)^2}\frac{x^2(1+x^2)^p}{x^4(1+x^2)^{2p}+\Omega^2}dx \qquad (8)$$

with the reduced frequency

$$\Omega = \frac{\omega}{\omega_D} = \omega/(\omega_0 t^{z\tilde{\nu}}) \qquad (9)$$

In the expression for the scaling function (eq 8) $p = 0.5$ for three-dimensional systems like the surfactant solutions.

In the following the measured spectra of the C_iE_j/water mixtures will be analytically represented by model relaxation spectral functions $R_m(\nu)$ which are composed of the background contribution $B\nu$ and, depending on the C_iE_j/water system, of a $R_H^{\#}$ term, a R_{BF} term, and R_D terms. Each model function has been fitted to the measured spectra using a nonlinear least-squares regression analysis[25] that minimizes the variance

$$\chi^2 = \frac{1}{N-J-1}\sum_{n=1}^{N}\left(\frac{(\alpha\lambda)_n - R_m(\nu_n,P_j)}{\Delta(\alpha\lambda)_n}\right)^2 \qquad (10)$$

The P_j, $j = 1, ..., J$ are the unknown parameters of $R_m(\nu)$ and the ν_n, $n = 1, ..., N$ denote the frequencies of measurements; $(\alpha\lambda)_n$ and $\Delta(\alpha\lambda)_n$ are the absorption-per-wavelength data at ν_n and their absolute experimental error, respectively. The inverse errors $\Delta(\alpha\lambda)^{-1}$ are used as weighing factors in the variance. The integral (eq 8) defining the Bhattacharjee−Ferrell scaling function $F(\Omega)$ has been calculated at 900 points using the

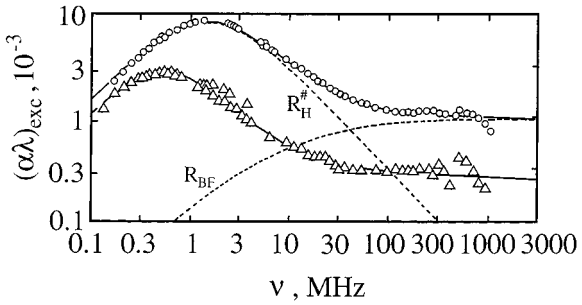

Figure 2. Ultrasonic excess absorption spectra of C_6E_5/H_2O mixtures with mass fraction $Y = 0.04$ (Δ) and $Y = 0.059$ (○) at 25 °C. For the mixture with higher surfactant content the dashed curves show a restricted Hill relaxation term $R_H^{\#}$ (eq 5) and a Bhattacharjee−Ferrell relaxation term R_{BF} (eq 6) as following from the regression analysis of the former spectrum. The full curve represents the sum of these terms.

Romberg method.[26] The integral has been interpolated between these points in the numerical calculations.

C_6E_4, C_6E_5, and C_7E_3. In Figure 2 excess absorption spectra of the C_6E_5/water system at 25 °C are displayed for two concentrations. These spectra resemble those for the C_6E_3/water mixtures at $Y > Y_{cmc}$.[8] At around 1 MHz a relative maximum in the $(\alpha\lambda)_{exc}$ data emerges. The relaxation process corresponding with this maximum turns out to be subject to a relaxation time distribution. It can be well represented by a restricted Hill term (eq 5) and is attributed to the monomer exchange between micelles and the suspending phase. The amplitude of this Hill-type relaxation contribution to the spectra (Figure 2) increases with surfactant concentration, in qualitative agreement with the Teubner−Kahlweit theory of ultrasonic absorption due to the kinetics of micelle formation.[24,27,28] At $c >$ cmc this theoretical model predicts an amplitude A_{mon} for the monomer exchange process which is given by

$$A_{mon} = \frac{\pi(\Delta V)^2 \text{cmc}}{\kappa_s^{\infty} RT} \frac{(\sigma^2/\bar{m})X}{1 + (\sigma^2/\bar{m})X} \tag{11}$$

where

$$X = (\text{c} - \text{cmc})/\text{cmc} \tag{12}$$

denotes the reduced concentration. In eq 11 ΔV is the reaction volume associated with the monomer exchange. It is assumed to be independent of the size of the micelles. Within the framework of the Teubner−Kahlweit model a Gaussian distribution of micelle sizes around a mean aggregation number $\bar{m}$ and with variance σ^2 is presumed. Further in eq 11, κ_s^{∞} is the adiabatic compressibility, extrapolated to high frequencies, of the liquid and R is the gas constant. Assuming $(\sigma^2/\bar{m})X \ll 1$ for the spectra shown in Figure 2, eq 11 yields $A_{mon}(Y{=}0.059)/A_{mon}(Y{=}0.04) \approx 2.1$ whereas $A_H^{\#}(Y{=}0.059)/A_H^{\#}(Y{=}0.04) \approx 3$ follows from an inspection of the spectra. Toward high frequencies the $(\alpha\lambda)_{exc}$ values of the C_6E_5/water system are nearly constant. A Bhattacharjee−Ferrell relaxation term can appropriately account for this behavior (Figure 2). Hence the ultrasonic absorption data of the C_6E_5/water mixtures have been represented by the model spectral function

$$R_m(\nu) = R_H^{\#}(\nu) + R_{BF}(\nu) + B\nu \tag{13}$$

This relaxation spectral function applies also for the spectra of the C_6E_4 and C_7E_3 systems. For the latter this statement is confirmed by Figure 3, where absorption data measured for the mixture with mass fraction $Y = 0.08$ along with the graphs of the theoretical model are displayed in the format $\alpha\nu^2$ vs ν. In this format the model spectral function reads

$$\frac{R_m(\nu)}{c_s\nu} = \frac{R_H^{\#}(\nu)}{c_s\nu} + \frac{R_{BF}(\nu)}{c_s\nu} + \frac{B}{c_s} \tag{14}$$

The parameter values for $R_m(\nu)$ as obtained from the nonlinear regression analysis are presented in Table 3. The amplitude of the restricted Hill term of the C_7E_3/water spectra is too small to allow for a clear statement about the width of its underlying relaxation time distribution. We therefore fixed the distribution parameter at $s_H = 1$. Hence the Hill term was treated as a Debye term with discrete relaxation time, in conformity with the extended Teubner−Kahlweit model at $Y \gg Y_{cmc}$.[24] It is worthwhile to notice that the C_7E_3/water spectra, within the limits of experimental error, are nicely represented by only five adjustable parameters if the $R_m(\nu)$ function (eq 13) is applied. In contrast, the attempt has failed to describe the spectra by nine adjustable parameters when using the sum of four Debye terms and the high-frequency asymptotic term (Figure 1).

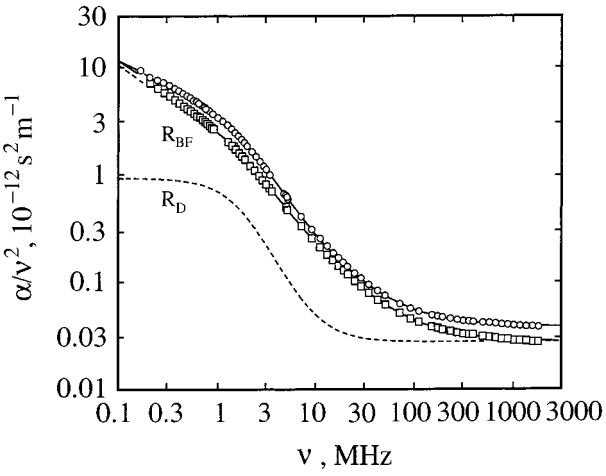

Figure 3. Ultrasonic spectra in the format α/ν^2 vs ν for the C_7E_3/H_2O mixture with mass fraction $Y = 0.08$ at $T = 12$ °C (○) and $T = 22.5$ °C (□). The full curves are the graphs of the relaxation spectral function with parameter values following from the fitting procedure (Table 3). Dashed curves show the subdivision of the spectrum at 22.5 °C in a Debye term R_D (eq 4, $R_D = R_H^{\#}$ at $s_H \equiv 1$) and a Bhattacharjee−Ferrell term (eq 6).

TABLE 3: Parameter Values of the Model Relaxation Spectral Function $R_m(\nu)$ Defined by Eq 13 as Obtained from the Nonlinear Least-Squares Regression Analysis of the Ultrasonic Absorption Spectra for C_6E_4/H_2O, C_6E_5/H_2O, and C_7E_3/H_2O Mixtures at Different Mole Fractions Y of Surfactant and Temperatures T[a]

Y, 10^{-2}	T, °C	$A_H^{\#}$, 10^{-3} ±5%	τ_H, ns ±5%	s_H ±5%	A_{BF}, 10^{-3} ±10%	ω_D, 10^6 s^{-1} ±20%	B, 10^{-12} s ±0.5%
C_6E_4, $Y_{cmc} = 0.02$, $Y_{crit} = 0.164$, $T_{crit} = 66.3$ °C							
8.0	17.5	24.5	46	0.73	15.5	202	44.40
	25.0	19.2	33	0.73	14.3	176	35.40
	32.5	14.8	27	0.80	10.2	33	30.24
	40.0	13.1	24	0.79	12.4	77	27.00
C_6E_5, $Y_{cmc} = 0.023$, $T_{crit} = 78.4$ °C							
4.0	25	5.3	297	0.87	1	7	33.60
5.9	25	16.3	110	0.70	3.7	32	34.55
C_7E_3, $Y_{cmc} = 0.006$, $Y_{crit} = 0.08$, $T_{crit} = 22.8$ °C							
8.0	12.0	5.4	98	1*	8.6	0.4	57.46
	19.0	3.6	98*	1*	8.2	0.5	46.30
	21.0	2.6	95	1*	8.5	0.4	44.24
	22.5	2.2	98	1*	8.6	0.3	43.02

[a] The asterisk indicates data that have been fixed.

TABLE 4: Parameter Values of the $R_m(\nu)$ Function (Eq 15) as Obtained from the Fitting Procedure of the Spectra for the System C_8E_5 at 25 °C and Different Mass Fractions Y of Surfactant; $Y_{cmc} = 0.0035$, $Y_{crit} = 0.096$, $T_{crit} = 59.6$ °C

Y, 10^{-2}	$A_H^{\#}$, 10^{-3} ±5%	τ_H, *ns* ±10%	s_H ±5%	A_{BF}, 10^{-3} ±10%	ω_D, $10^6\ s^{-1}$ ±50%	A_{Duh}, 10^{-3} ±25%	τ_{Duh}, *ns* ±20%	B, 10^{-12} *s* ±0.5%
0.37	0.19	1380	≡1	–	–	–	–	32.26
4.74	3.4	104	0.65	5.9	337	1.9	0.19	35.0
6.81	3.2	108	0.38	3.9	71	3.5	0.25	37.22
9.07	3.6	109	0.28	7.0	138	4.1	0.24	38.67

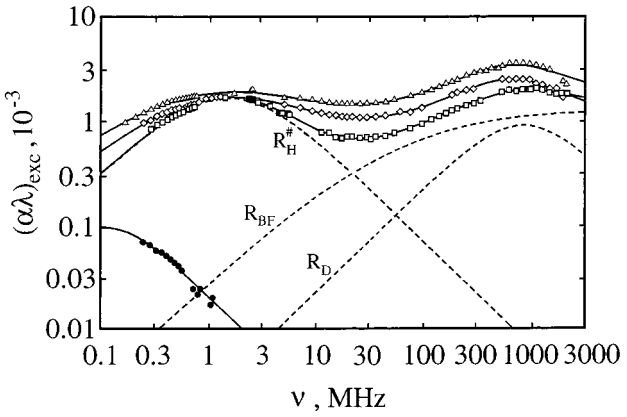

Figure 4. Ultrasonic excess absorption spectra for C_8E_5/H_2O mixtures at 25 °C with mass fraction $Y = 0.0037$ (●), 0.047 (□), 0.068 (◇), and 0.091 (△). Full curves are the graphs of the relaxation spectral functions used to represent the measured data, with parameter values as following from the least-squares fitting procedure (Table 4). Dashed curves show the contributions from different relaxation terms for the $Y = 0.047$ mixture.

C_8E_5. In Figure 4 the ultrasonic absorption spectra of the C_8E_5/water systems at different surfactant contents are displayed at 25 °C. Even though our measuring range does not extend to sufficiently small frequencies to enable a complete characterization of the spectrum for the solution with smallest surfactant concentration ($Y = 0.0037$), sonic absorption with relaxation characteristics emerges already at this Y ($\approx Y_{cmc}$). This relaxational behavior is due to the formation/decay of oligomeric species rather than proper micelles.[24] At higher surfactant content the low-frequency relaxation reflects the monomer exchange between proper micelles and the suspending phase. With the C_8E_5/water system the restricted Hill term representing this part of the spectrum is rather broad (Figure 4). Correspondingly, the *s* parameter is unusually small. Obviously it decreases with Y (Figure 4). As will be discussed below (Figure 5) for the C_8E_4/water system, this spectral range can no longer be described by one relaxation term with continuous relaxation time distribution but has to be represented by a sum of two separate terms. In contrast to the spectra for the mixtures of C_6E_3, C_6E_4, and C_7E_3 with water, the high-frequency part of the C_8E_5/water spectra does not only reflect a Bhattacharjee−Ferrell term. At around 1 GHz a relative maximum points at an additional Debye-type relaxation term. Consequently, the model spectral function

$$R_m(\nu) = R_H^{\#}(\nu) + R_{BF}(\nu) + R_{Duh}(\nu) + B\nu \qquad (15)$$

has been applied to the C_8E_5/water spectra. The parameters of this function are displayed in Table 4. It turns out that Debye relaxation processes add contributions to the ultrasonic spectra of the C_iE_j/water mixtures in significantly different frequency regions. We therefore discriminate the different spectral regions of these terms: uh, "ultra high", 200 ps ≤ τ_{Duh} ≤ 500 ps; *h*, "high", 2 ns ≤ τ_{Dh} ≤ 10 ns; l, "low", 80 ns ≤ 160 ns; vl, "very low", 0.4 μs ≤ τ_{Dvl} ≤0.9 μs.

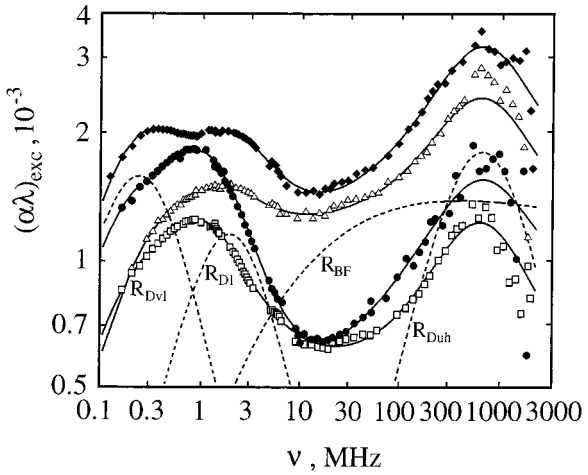

Figure 5. Ultrasonic excess absorption spectra for C_8E_4/H_2O mixtures: ●, $Y = 0.035$, 17.5 °C; □, $Y = 0.035$, 32.5 °C; ◆, $Y = 0.071$, 17.5 °C; Δ, $Y = 0.071$, 32.5 °C. Full curves show the results of the regression analysis using a model spectral function (eq 16) that contains a Bhattacharjee−Ferrell and three Debye-type relaxation terms. The dashed curves indicate the contributions from the individual terms.

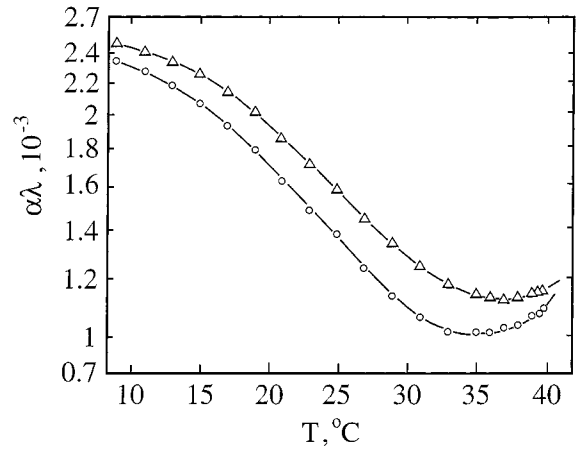

Figure 6. Absorption per wavelength as a function of temperature for the C_8E_4/H_2O mixtures with mass fraction $Y = 0.071$ at $\nu = 210$ (○) and 320 kHz (△). The demixing temperature is $T_{crit} = 39.8$ °C. The curves are drawn to guide the eye.

C_8E_4. The C_8E_4/water mixtures appear to be even more complex than the C_8E_5/water mixtures. As shown in Figure 5 by the spectrum for the composition $Y = 0.071$ and the temperature $T = 32.5$ °C, there may be up to three relative maxima in the $(\alpha\lambda)_{exc}$ data, indicating that at least three Debye relaxation terms are required for an analytical representation. A detailed analysis of the measured spectra reveals also contributions from concentration fluctuations. Their existence has been verified by measurements of the ultrasonic absorption coefficient at fixed frequencies as a function of temperature. The series of data presented in Figure 6 for the mixture of critical composition show that, contrary to the temperature behavior of the background contributions, the $(\alpha\lambda)_{exc}$ values increase when approaching T_{crit}, thus pointing at a critical part in α. Therefore,

TABLE 5: Parameter Values of the Model Relaxation Spectral Function $R_m(\nu)$ Given by Eq 16 as Following from the Nonlinear Regression Analysis of the Ultrasonic Spectra for the C_8E_4/Water Mixtures at Two Mass Fractions Y of Surfactant and at Four Temperatures T[a]

T, °C	A_{Dvl}, 10^{-3} ±10%	τ_{Dvl}, ns ±10%	A_{Dl}, 10^{-3} ±10%	τ_{Dl}, ns ±10%	A_{BF}, 10^{-3} ±5%	ω_D, 10^6 s^{-1} ±25%	A_{Duh}, 10^{-3} ±10%	B, 10^{-12} s ±0.5%
				Y=0.035				
17.5	1.8	822	2.8	149	3.0	55	1.5	43.28
25.0	1.2	661	2.0	157	1.9	10	1.9	33.71
32.5	1.0	761	1.5	157	1.7	4	1.4	27.91
39.0	1.2	761*	1.2	157*	2.0	4	1.5*	24.90
				Y=0.071				
17.5	3.1	667	2.3	83	5.2	17	3.6	47.15
25.0	1.9	493	1.2	93	4.1	4	3.2	37.87
32.5	1.2	491	1.2	107	4.1	5	2.5	32.02
39.0	1.0	491*	0.6	107*	4.1*	2	2.5*	29.93

[a] The relaxation time of the ultrahigh frequency Debye term has been fixed at $\tau_{Duh} = 0.25$ ns throughout. The asterisk indicates data that have been also fixed in the fitting procedure. $Y_{cmc} = 0.002$, $Y_{crit} = 0.071$, $T_{crit} = 39.8$ °C.

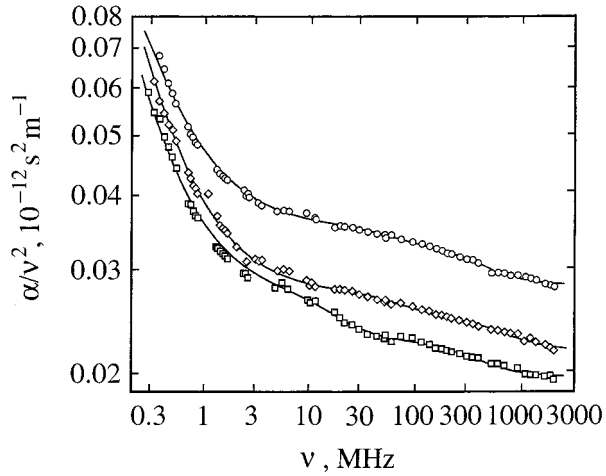

Figure 7. Ultrasonic absorption spectrum in the format α/ν^2 vs ν for the $C_{12}E_5/H_2O$ mixture with mass fraction $Y = 0.015$ at 17.5 (○), 25 (□), and 29.4 °C (◇). The curves are graphs of the spectral function defined by eq 22 with the parameter values given in Table 6.

the suitable model relaxation function for the C_8E_4/water system reads

$$R_m(\nu) = R_{Dvl}(\nu) + R_{Dl}(\nu) + R_{BF}(\nu) + R_{Duh}(\nu) + B\nu \quad (16)$$

The parameters of $R_m(\nu)$ as derived from the fitting procedure are collected in Table 5.

$C_{10}E_4$ and $C_{12}E_5$. As illustrated by the examples given in Figure 7, the ultrasonic absorption of the mixtures of longer nonionic surfactants is small and it is dominated by a monotonous increase of the α/ν^2 data toward lower frequencies. According to the Teubner−Kahlweit model,[27,28] the relaxation time

$$\tau_{mon} = \frac{1}{k^b}\left(\frac{1}{\sigma^2} + \frac{X}{\bar{m}}\right)^{-1} \quad (17)$$

of the monomer exchange process is so large that the corresponding relaxation process is located at the lower frequency limit of our measuring range. In eq 17 k^b denotes a particular backward rate constant of the isodesmic reaction scheme[29−30]

$$N_1 + N_{i-1} \underset{k^b_i}{\overset{k^f_i}{\rightleftharpoons}} N_i, \quad i = 2,..., N \quad (18)$$

underlying the theoretical model of micelle formation. Applying this scheme of coupled chemical equilibria $k^b_i \approx k^b_{i+1}$ is assumed around the maximum of the Gaussian distribution of micellar sizes[27,28] and k^b is taken as this almost size independent value ($k^b = k^b_{\bar{m}}$).

In order to reduce the number of unknown parameters in the fitting procedure, a Debye-type relaxation process has been assumed for the $C_{10}E_4$/water spectra ($s_H \equiv 1$ in eq 5, hence $R_H^{\#}(\nu) \rightarrow R_{Dvl}(\nu)$) and the relaxation time τ_{Dvl} has been fixed at an estimated value of 0.7 μs. Due to the small cmc of the $C_{12}E_5$/water system, contributions from the monomer exchange to its spectra have been neglected at all ($A_{mon} \rightarrow 0$ if cmc $\rightarrow 0$, eq 11). Neither the shape of the ultrasonic absorption spectra nor their dependence upon temperature yields indications for contributions from concentration fluctuations. Obviously, only at frequencies below our measuring range do critical phenomena add contributions to the sonic spectra. For consistency with the results for solutions of shorter C_iE_j, we nevertheless considered a Bhattacharjee−Ferrell term in the description of the ultrasonic absorption data. We fixed, however, the characteristic frequency ω_D of this term at the values following from the relation[21,22]

$$\omega_D = \omega_0 t^{z\tilde{\nu}} = \frac{k_B T}{3\pi\eta_0 \xi_0^3} t^{z\tilde{\nu}} \quad (19)$$

Herein k_B is Boltzmann's constant, ξ_0 is the amplitude of the correlation length (eq 1, Table 1), and η_0 is the viscosity amplitude, defined by the temperature dependence

$$\eta_s(T) = \eta_0 t^{-(z-3)\tilde{\nu}} \quad (20)$$

of the shear viscosity η_s close to T_{crit}. This treatment of the spectra turned out to be useful because it allows for an intercomparison of the Bhattacharjee−Ferrell amplitude of all C_iE_j/water systems under consideration.

There is evidence for two further contributions with relaxational characteristics to the spectra for the solutions of longer surfactants. Due to the small amplitudes of these contributions, however, no statements can be made on possibly underlying relaxation time distributions. Hence we assumed simple Debye-type processes and applied the model spectral functions

$$R_m(\nu) = R_{Dvl}(\nu) + R_{BF}(\nu) + R_{Dh}(\nu) + R_{Duh}(\nu) + B\nu \quad (21)$$

and

$$R_m(\nu) = R_{BF}(\nu) + R_{Dh}(\nu) + R_{Duh}(\nu) + B\nu \quad (22)$$

to the $C_{10}E_4$/water and $C_{12}E_5$/water spectra, respectively. The parameter values for these functions are presented in Table 6.

TABLE 6: Parameter Values of the Model Spectral Functions Defined by Eqs 21 and 22 as Obtained from the Regression Analysis of the Ultrasonic Absorption Spectra for the $C_{10}E_4$/Water System ($Y = 0.02$) and the $C_{12}E_5$/Water System ($Y = 0.015$), Respectively[a]

T, °C	A_{Dvl}, 10^{-3} ±10%	A_{BF}, 10^{-3} ±10%	ω_D, 10^6 s^{-1}	A_{Dh}, 10^{-3} ±10%	τ_{Dh}, *ns* ±10%	A_{Duh}, 10^{-3} ±10%	τ_{Duh}, *ns* ±10%	B, 10^{-12} *s* ±0.5%
			$C_{10}E_4$, $Y_{cmc} = 0.000\ 27$, $Y_{crit} = 0.02$, $T_{crit} = 18.2$ °C					
12.0	0.27	0.12	86*	0.34	7.8	2.4	0.4*	50.63
14.0	0.23	0.14	41*	0.27	9.1	2.8	0.4*	45.70
16.0	0.16	0.17	12*	0.36	5.5	2.0	0.4*	44.20
18.0	0.07	0.22	0.12*	0.26	8.2	2.6	0.4*	40.50
			$C_{12}E_5$, $Y_{cmc} = 0.000\ 039$, $Y_{crit} = 0.015$, $T_{crit} = 29.6$ °C					
17.5	–	0.050	103*	0.22	2.8	2.7	0.38	41.09
25.0	–	0.043	16*	0.27	2.2	2.9	0.23	31.95
29.4	–	0.033	0.04*	0.11	9.4	1.6	0.43	30.09

[a] For the $C_{10}E_4$/water system the relaxation time of the very-low-frequency Debye term has been fixed at $\tau_{Dvl} = 700$ ns. Data marked by an asterisk have been also fixed in the fitting procedure.

4. Discussion

Asymptotic High-Frequency Absorption; Shear Viscosity Relaxation. The asymptotic high frequency ultrasonic absorption (eq 3) reflects attenuation mechanisms due to viscous friction and heat conduction of the sample. For nonmetallic liquids the latter effect is small as compared to the former. Hence the contribution from the final heat conductivity is normally neglected and the B coefficient of the asymptotic high-frequency contribution to the absorption per wavelength (eq 3) is related to the shear viscosity as[31,32]

$$B = \frac{2\pi^2}{\rho c_s^2}\left(\frac{4}{3}\eta_s + \eta_v\right) \tag{23}$$

Here η_s is the shear viscosity at the highest frequencies of the measuring range and η_v is the volume viscosity at the same frequencies. η_v is related to the curl-free part of the sonic field. B may contain contributions from relaxation mechanisms with relaxation frequencies above the measuring range. If such mechanisms are absent

$$\eta_v/\eta_s = {}^2/_3 \tag{24}$$

is predicted from theoretical considerations.[33,34] Measurements of liquid nobel gases confirm this value of the viscosity ratio, whereas $\eta_v/\eta_s = 2.68$ for water at room temperature. This considerable η_v/η_s value of the associating liquid is an indication for the existence of a high-frequency structure relaxation.

For reasons of comparison the shear viscosity values η_s ($=\eta_s(\nu\rightarrow 0)$) of the aqueous C_iE_j solutions (Table 1) are plotted versus temperature in Figure 8. Also given in that diagram are the water data,[35] values for the C_6E_3/water system,[8,36] and additional values for the C_8E_4/H_2O mixture of critical composition.[37] The η_s values for the aqueous solutions of shorter C_iE_j, similar to those for water itself, decrease with T. They increase with surfactant concentration. The data for the C_7E_3/water and the C_8E_4/water systems slightly increase when T approaches the critical temperature, in conformity[37] with the theoretical predictions (eq 20). The solutions of longer C_iE_j exhibit a strong increase in the shear viscosity at rising temperature. The same behavior has been already found previously[19] and has been assigned to structural changes of the micelles. A transition from almost globular to extended (prolate ellipsoidally or tubularly shaped) micelles could be the reason for the unusual temperature dependence of the viscosity.

Despite the high shear viscosities the B values for the $C_{10}E_4$/water and $C_{12}E_5$/water systems are small (Table 6) and close to the B values for water at the same temperature, respectively.

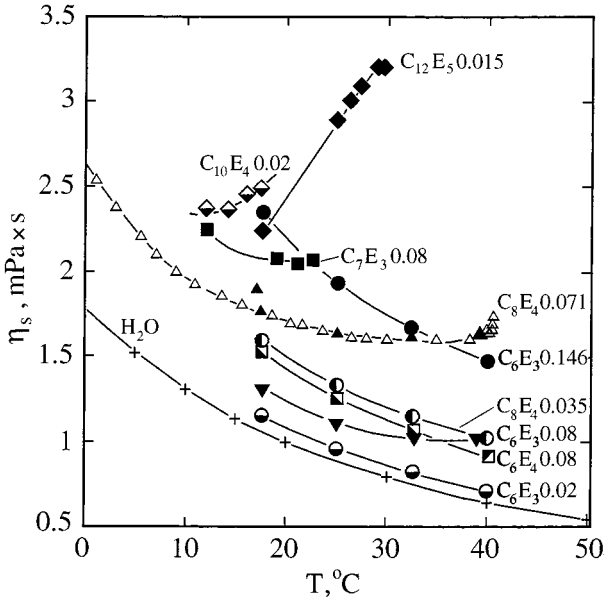

Figure 8. Static shear viscosity of the C_iE_j/water mixtures with mass fraction Y displayed as a function of temperature. Pure water data[35] and η_s values for the C_6E_3/H_2O system[8] have been taken from the literature.

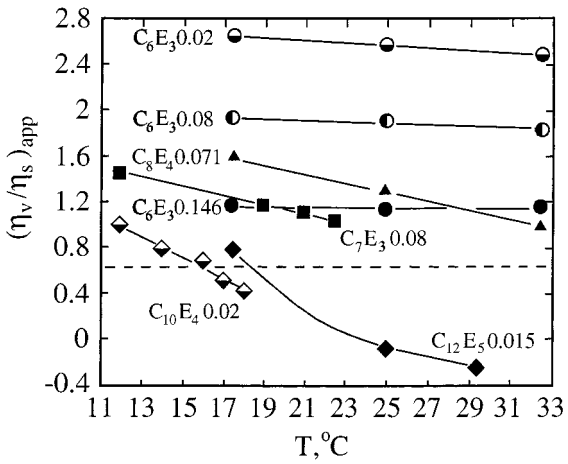

Figure 9. Apparent volume viscosity-to-shear viscosity ratio versus temperature for some C_iE_j/water systems, including C_6E_3/H_2O.[8] The dashed line represents the limiting value $^2/_3$ (eq 24).

Consequently, the apparent η_v/η_s ratios for these systems toward higher temperatures become smaller than the limiting value (eq 24) and even negative values are found (Figure 9). The $(\eta_v/\eta_s)_{app}$ data have been calculated from the (static) shear viscosities

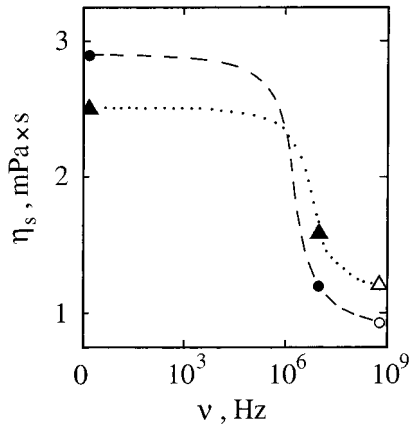

Figure 10. Shear viscosity as a function of frequency of the $C_{10}E_4$/water mixture with $Y = 0.02$ at 17 °C (triangles) and the $C_{12}E_5$/water system with $Y = 0.015$ at 25 °C (points/circle). The static η_s values have been measured with a falling ball viscometer, the data at 10 MHz with a shear impedance spectrometer.[38] The high-frequency data (open symbols) result from an evaluation of the asymptotic high-frequency contribution to the ultrasonic spectrum (eq 23).

$\eta_s(\nu\rightarrow 0)$ using eq (23). The finding of extraordinarily small $(\eta_\nu/\eta_s)_{app}$ data indicates a dispersion in the shear viscosity of the long chain surfactant systems. Utilizing a shear impedance spectrometer,[38] we therefore measured at frequencies between 6 and 20 MHz the shear viscosity of the $C_{10}E_4$/water mixture at 17 °C and that of the $C_{12}E_5$/water system at 25 °C. We found $\eta_s(\nu=10$ MHz) values distinctly smaller (Figure 10) than the static values $\eta_s(\nu\rightarrow 0)$. Let us assume the (real) η_ν/η_s ratios for the $C_{10}E_4/H_2O$ and for the $C_{12}E_5/H_2O$ mixtures, due to the small surfactant concentration, to resemble those of water. This assumption seems to be justified by the apparent viscosity ratios of the C_6E_3/water system with $Y = 0.02$ (Figure 9), which are very close to those for water at the same temperature ($\eta_s/\eta_s = 2.68$, water, 25 °C). If this assumption is accepted, we can calculate the shear viscosity $\eta_s(\nu=1$ GHz) at around 1 GHz from the B values of the ultrasonic spectra. These $\eta_s(1$ GHz) data, also shown in Figure 10, may be taken to confirm our idea of a shear viscosity relaxation in the present frequency range of ultrasonic measurements. This idea is also supported by recent results from ultrasonic (100 kHz to 5 GHz) and shear impedance (20 MHz to 120 MHz) spectrometry of long-chain alkanes and alcohols, which yielded also a shear viscosity relaxation.[38] Viscoelastic behavior of concentrated $C_{12}E_6$/water mixtures has been also inferred from ultrasonic attenuation spectrometry in the frequency range 5−155 MHz.[39] Here we got direct evidence of a shear viscosity relaxation in solutions of long-chain poly(ethylene glycol) monoalkyl ethers from the addditional shear impedance measurements (Figure 10). A full enlightenment of the viscosity behavior of long-chain C_iE_j systems, however, requires further broad-band shear impedance measurements.

The $(\eta_\nu/\eta_s)_{app}$ ratio of the other C_iE_j/water systems shows the normal characteristics (Figure 9). It decreases with solute content, indicating that the particular voluminous water structure significantly changes with increasing surfactant concentration. There is also a tendency toward lower $(\eta_\nu/\eta_s)_{app}$ values at higher temperatures where the effects from the special water properties are smaller than at lower temperatures.

Monomer Exchange. For some C_iE_j/water systems the relaxation rates τ_H^{-1} of the Hill-type relaxation term, assigned to the monomer exchange process in the micelle formation/decay kinetics, are displayed versus $X/\bar{m}$ in Figure 11. The plots shown in this figure reveal three $X/\bar{m}$ regions of different solution behavior. Above the concentration range around the cmc ($X/\bar{m}$ > 0.02), up to $X/\bar{m} \approx 0.1$, the concentration dependence of the relaxation rate is in conformity with the predictions of the Teubner−Kahlweit model which yields a linear dependence of τ_H^{-1} upon $X/\bar{m}$ (eq 17, $\tau_H = \tau_{mom}$). From the slopes of the τ_H^{-1} versus $X/\bar{m}$ relations plotted in Figure 11, k^b values between 0.1×10^9 s^{-1} (C_8E_4/water, 25 °C) and 0.6×10^9 s^{-1} (C_6E_3/water, 25 °C) result.

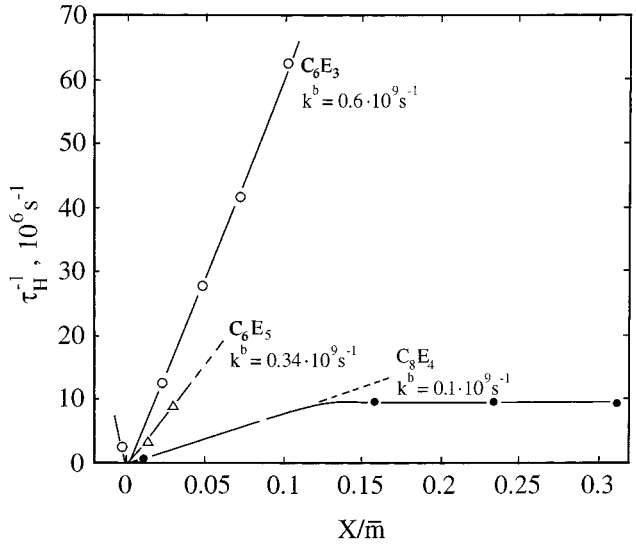

Figure 11. Relaxation rate $1/\tau_H$ of the restricted Hill term vs parameter $X/\bar{m}$. Dashed curves are graphs of the predictions from the Teubner−Kahlweit theory for the monomer exchange process (eq 17).

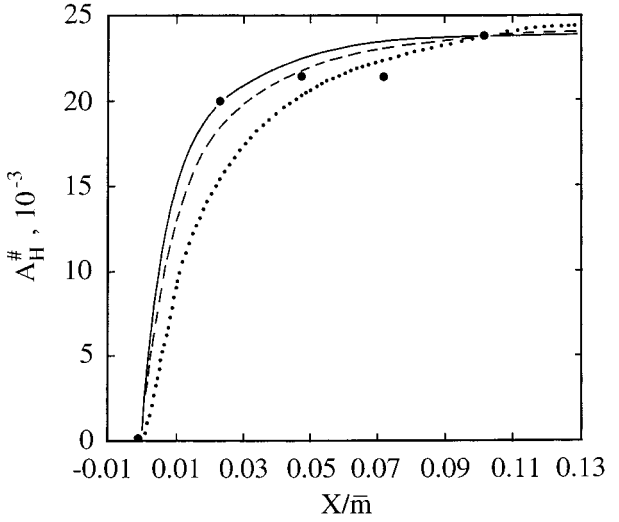

Figure 12. Hill term amplitude $A_H^{\#}$ of the C_6E_3/H_2O mixture at 17.5 °C displayed versus $X/\bar{m}$. The curves show the predictions of the Teubner−Kahlweit model (eq 11) for different widths of the (Gaussian) size distribution of micelles: full curve, $\sigma^2 = 50$; dashed curve, $\sigma^2 = 100$; dotted curve, $\sigma^2 = 150$.

At around the cmc, deviations from the linear dependence of the relaxation rate τ_H^{-1} upon the reduced concentration may occur, as indicated by the C_6E_e/water system (Figure 11). Such deviations have been especially found for systems with high critical micelle concentration, such as *n*-heptylammonium chloride (cmc = 0.45 mol/L, 25 °C[23]) and *n*-hexylammonium chloride (cmc = 0.9 mol/L, 25 °C[40]), and have been attributed to the formation/decay kinetics of premicellar oligomeric species. At $c <$ cmc this oligomer region exhibits a negative slope in the τ_H^{-1} versus $X/\bar{m}$ relation.

Deviations from the Teubner−Kahlweit model (eq 17) at higher surfactant content ($X/\bar{m} > 0.1$, Figure 11) are due to

TABLE 7: Reaction Volume ΔV of the Monomer Exchange Process, Calculated According to Eq 25 for C_iE_j/Water Mixtures with Critical Micelle Concentration cmc

surfactant	T, °C	cmc, 10^{-3} mol/L	ΔV, cm^3/mol
C_6E_3	17.5	98	8.8
	25	92	7.8
	32.5	86	7.2
	40	82	6.6
C_6E_4	17.5	93	9.5
	25	80	9.1
	32.5	65	8.8
	40	60	8.7
C_6E_5	25	73	8.7
C_7E_3	12	23	9.0
	19	23	7.4
	21	23	6.3
	22.5	23	5.8
C_8E_4	17.5	9.0	10.9
	25	7.6	9.2
	32.5	7.0	7.7
	39	6.8	7.1
C_8E_5	25	9.2	11.7

interactions between micelles. The aggregates can no longer be considered isolated species in a solvent consisting of water and monomers (with concentration $c_1 = \text{cmc}$). Local fluctuations in the concentration and thus activity corrections have to be taken into account. In addition, changes in the micellar shape may affect the monomer exchange at high surfactant concentrations.

In Figure 12, as an example, the relaxation amplitude $A_H^{\#}$ of the C_6E_3/water mixture at 17.5 °C is plotted versus $X/\bar{m}$. Also shown for three different widths σ^2 of the micellar size distribution function are graphs for the monomer exchange relaxation amplitude (eq 11). The $A_H^{\#}$ values from the measured spectra largely follow the trend given by the Teubner−Kahlweit relation (Figure 12). Because there do not exist experimental data in the $X/\bar{m}$ range between 0 and 0.02, no definite conclusions can be drawn on the width of the Gaussian size distribution function (Figure 12). Since, on the other hand, the constant plateau region at high $\sigma^2/\bar{m}$ (eq 11) is nearly reached by the measurements, we used the $A_{H\,\max}^{\#} = A_H^{\#}(X\rightarrow\infty)$ values at high surfactant concentration to calculate the reaction volumes of the C_iE_j/water system, using eq (11) in the format

$$\Delta V = \left(\frac{A_{H\,\max}^{\#}\kappa_s^{\infty}RT}{\pi(\text{cmc})}\right)^{1/2} \qquad (25)$$

The ΔV values following thereby are collected in Table 7. The $C_{10}E_4/H_2O$ mixture has been omitted here because of the small relaxation amplitude of the monomer exchange process.

The reaction volume is predominantly given by the difference in the hydration properties of the monomers and the C_iE_j molecules incorporated in micelles. Hence it mainly reflects the reduction of the clathrate-like hydrophobic hydration region around the hydrocarbon chain, when the surfactant enters a micellar aggregate. Since the voluminous hydrogen bond structure of water successively breaks down with rising temperature, the reaction volume decreases with T. As a first approximation the ΔV values of a C_iE_j molecule might be considered a simple sum

$$\Delta V = \Delta V_{CH_3} + (i-1)\,\Delta V_{CH_2} + j\Delta V_E \qquad (26)$$

of volume changes that are ascribed to the terminal CH_3 group, the CH_2 groups, and the ethylene oxide groups (E) of the nonionic surfactants. If this is accepted, the difference in the ΔV values of C_8E_5 and C_6E_5 result in $\Delta V_{CH_2} = 1.5$ mL/mol (25 °C) and the difference in the reaction volumes of C_8E_5 and C_8E_4 yields $\Delta V_E = 2.4$ mL/mol (25 °C). These data, however, do not allow for a consistent description of the set of reaction volumes (Table 7). With the C_6E_3/water system, for example, $\Delta V = \Delta V_{CH_3} + 14.7$ mL/mol, as calculated with the aid of eq 26, is distinctly larger than the value 7.8 mL/mol derived from the relaxation amplitude data (eq 25, Table 7). There may be several reasons for this discrepancy. Let us just mention the following, probably most important ones. In view of the complex interplay of a variety of factors in the hydration properties of a molecule, the linear superposition of hydration effects (eq 26) from different parts of the surfactant is doubtless an oversimplification. In addition, the ΔV data derived from the Hill term amplitudes depend on the cmc of the system (eq 25) which is a concentration range rather than a definite value.

TABLE 8: Characteristic Frequency ω_D of Critical Concentration Fluctuations, as Taken from the Ultrasonic Spectra (Tables 3−5) on the one Hand and as Calculated According to Eq 19 on the Other Hand, for the C_iE_j/Water Mixtures at Reduced Temperature t, as well as Characteristic Frequency Amplitude ω_0 Assumed To Be Independent of Temperature

surfactant	T, °C	t, 10^{-2}	ω_D (Tables 3−5) $10^6\ s^{-1}$	ω_D(eq 19) $10^6\ s^{-1}$	ω_0, $10^9\ s^{-1}$
C_6E_3	17.5	8.93	61 ± 1.6	71	7.38
	25	6.58	39 ± 6	40	
	32.5	4.23	15.9 ± 1.3	17	
	40	1.88	4.8 ± 0.6	3.6	
C_7E_3	12	3.65	0.42 ± 0.03	4.0	2.30
	19	1.28	0.48 ± 0.06	0.54	
	21.5	0.61	0.37 ± 0.04	0.13	
	22.5	0.10	0.29 ± 0.04	0.004	
C_8E_4	17.5	7.13	17 ± 3	11	1.75
	25	4.73	4.3 ± 0.1	5	
	32.5	2.33	4.7 ± 0.1	1.3	
	39	0.26	1.9 ± 0.2	0.019	
$C_{10}E_4$	12	2.13		0.083	0.14
	14	1.44		0.041	
	16	0.76		0.012	
	18	0.069		0.001	
$C_{12}E_5$	17.5	4.0		0.103	0.05
	25	1.52		0.016	
	29.4	0.066		0.00004	

Critical Fluctuations. There clearly exist contributions from concentration fluctuations in the ultrasonic absorption spectra. This result of our measurements becomes particularly obvious in the intercomparison of spectra for the C_6E_3/water system and the C_6E_4/water system[8] since the critical temperatures of these binary liquids are significantly different from another. The critical contribution is also inferred from the series of α-data at fixed frequency measured as a function of temperature (Figure 6). With many C_iE_j/water spectra, however, the contributions from concentration fluctuations to the C_iE_j/water spectra, however, is largely masked by those from the monomer exchange process. We therefore used the phenomenological "classical" Bhattacharjee−Ferrell theory and did not additionally apply recently published more specific models.[41−45]

The applicability of the Bhattacharjee−Ferrell theory may be examined by comparison of the experimental characteristic frequency data with the predictions of eq 19. In doing so ξ_0 values from Table 1 have been used and η_0 values have been estimated from the η_s data of the mixtures (Table 2). In addition, in order to obtain temperature-independent ω_0 values, $T = T_c$ has been taken. The resulting ω_0 and ω_D data and also the characteristic frequencies from the measured spectra are presented in Table 8. In the evaluation of the ultrasonic spectra for the $C_{10}E_4$/water and $C_{12}E_5$/water mixtures, the theoretical

TABLE 9: Critical Part $\tilde{A}$ of the Specific Heat at Constant Pressure and Amount $|g|$ of the Coupling Constant for the C_iE_j/Water Systems, Including $i-C_4E_1/H_2O$[49]

surfactant	$\tilde{A}$, $J\,kg^{-1}\,K^{-1}$	$\lvert g\rvert$
$i-C_4E_1/H_2O$	82.9	1.19
C_6E_3/H_2O	57.6	0.81
C_7E_3/H_2O	27.1	0.85
C_8E_4/H_2O	15.7	0.80
$C_{10}E_4/H_2O$	2.02	0.54
$C_{12}E_5/H_2O$	0.90	0.33

values had already been used as fixed parameters, in order to enhance the significance of the other parameters in the fitting procedure. With the C_6E_3/water mixture of critical composition, both sets of ω_D values almost perfectly agree with another. With the C_7E_3/water and C_8E_4/water systems, the agreement between the theoretical and the experimental ω_D data is less satisfactory, probably due to some interference of the critical contribution in the spectra with contributions from other mechanisms. Nevertheless, the order of magnitude of the experimental data agrees with the predictions from the Bhattacharjee−Ferrell theory.

According to

$$g = \tilde{B}/c_s(\hat{A}_{BF}T/(\pi\tilde{A}))^{1/2} \tag{27}$$

the amplitude $\hat{A}_{BF}$ of the Bhattacharjee−Ferrell term (eq 7) is related to the coupling constant g of the binary liquid of critical composition.[46] In eq 27 $\tilde{A}$ and $\tilde{B}$ are the critical contribution and the background part, respectively, of the specific heat c_p at constant pressure. Since there are no c_p data available, we utilized the relation

$$\xi_0\left(\frac{\tilde{\alpha}\tilde{A}\rho_{cr}}{k_B}\right)^{1/3} = R_\xi^+ = 0.27 \tag{28}$$

that follows from the two-scale-factor conception[47,48] to calculate $\tilde{A}$ values from the known ξ_0 and $\tilde{\alpha}$ data and from the density ρ_{cr} at the critical point. We used the c_p value for water (4185 J $kg^{-1}\,K^{-1}$) for the background part $\tilde{B}$ of the (water-rich) mixtures.

The $\tilde{A}$ and $|g|$ data of the present C_iE_j/water systems and also of the previously studied isobutoxyethanol/water mixture (i-C_4E_1/H_2O) of critical composition[49] are given in Table 9. It is realized that a noticeable contribution to the distinct dependence of the critical amplitude A_{BF} upon the surfactant molecule length originates from a corresponding dependence in the critical part $\tilde{A}$ of c_p. Another contribution results from a dependence of the coupling constant on the length of the C_iE_j molecules. The order of magnitude of the $|g|$ values for the C_iE_j/water systems is in accordance with coupling constants for other binary liquid mixtures.[46,50]

For the $C_{12}E_5$/water mixtures nonuniversal critical exponents have been found previously and high noncritical background contributions to the relaxation rate of the order parameter fluctuations have been reported.[51−53] These characteristics have been suggested to reflect effects from the nonvanishing size of the fluctuating micelles and have been discussed in terms of the dynamic droplet model. Dynamic light scattering measurements of mixtures of water with C_6E_3 and $C_{10}E_4$[54] as well as $C_{12}E_5$[55] are in conformity with this model. However, there does not exist a theory describing the ultrasonic properties of a liquid mixture in terms of the droplet model. In order to study the effect of the finite micellar size in the sonic spectra, we therefore substituted the scaling function $F(\Omega)$ in eq 6 by a modified version

$$\tilde{F}(\Omega) = \frac{3}{\pi}\int \frac{x^3}{(1+x^2)^2}\frac{\tilde{K}_{BF}(x,x_1)}{\tilde{K}_{BF}{}^2(x,x_1)+\Omega^2}\,dx \tag{29}$$

where $K_{BF}(x) = x^2(1+x^2)^p$ is exchanged by

$$\tilde{K}_{BF}(x,x_1) = \frac{\xi^2}{RD}\Gamma(x,x_1) \tag{30}$$

$R(\approx 1)$ is a dimensionless constant[56] and

$$\Gamma(x,x_1) = R\frac{k_BT}{6\pi\eta_sR_1}\frac{3\pi}{8}\frac{\bar{\Gamma}(3-\tau,x_1{}^{d_f})}{\bar{\Gamma}\left(3-\tau-\frac{1}{d_f},x_1{}^{d_f}\right)}\frac{\bar{\Gamma}\left(3-\tau-\frac{1}{d_f},u\right)}{\bar{\Gamma}(3-\tau,u)} \tag{31}$$

is the relaxation rate of the order parameter fluctuations within the droplet model. The dynamic droplet model is based on the assumption of a fractal nature of the mixture. It involves a minimum length $R_1 = x_1/k$ which is identified with the micellar radius here. Parameter d_f (=2.5) denotes the fractal dimension of the presumed clusters in the liquid mixture and τ (=2.2) is an exponent characterizing their size distribution. Furthermore

$$\bar{\Gamma}(a,y) = \int_y^\infty t^{a-1}e^{-t}\,dt \tag{32}$$

is the incomplete Gamma function and

$$u = (x_1/x)^{d_f}(1+x^2)^{d_f/2} \tag{33}$$

We found that the use of $\tilde{F}$ instead of the original F function does not noticeably alter the form of the predicted ultrasonic spectra. Only the dependence of the spectra upon the reduced temperature t is somewhat different for both scaling functions. Evident deviations, however, result only at temperatures distinctly apart from the critical, where the correlation length ξ is comparable with the minimum length R_1. Applying the modified scaling function in the regression analysis of the C_6E_3/water spectra resulted in ω_D values which, within the limits of errors, agreed with those obtained from the Bhattacharjee−Ferrell model.[8] The reason for the small effect of the finite micellar size may be the large ξ_0 value which, near T_c, leads to a small influence of the relevant quantity R_1/ξ. Hence, at least in the mixtures of water with the shorter C_iE_j, the effect of the nonvanishing micellar size in the critical sound absorption can be neglected.

Chain Isomerization. In the spectra of solutions of longer C_iE_j, an ultrahigh-frequency relaxation exists with a relaxation time τ_{uh} at around 0.25 ns (25 °C, Tables 4−6). Due to the small cmc of those systems, this relaxation is unlikely to reflect a monomer process. Special hydration effects have been discussed in the literature.[5] However, such effects should be also present in short-chain surfactant systems. In addition, dielectric spectrometry showed that the hydration water residence and reorientation times of similar molecules are smaller rather than 0.25 ns.[57,58] We therefore suggest the ultrahigh-frequency relaxation to reflect structural isomerizations of hydrocarbon chains within the micellar cores.

Previous broad-band ultrasonic studies on aqueous solutions of cationic, anionic, zwitterionic, and nonionic surfactants also revealed a high frequency relaxation process with relaxation time between 0.1 and 0.31 ns (Table 10[59,60]). This relaxation time does not show a noticeable dependence upon the cmc or the head group of the surfactant molecule. The assumption of

TABLE 10: Relaxation Time τ_{uh} of the Ultrahigh-Frequency Relaxation Process for Aqueous Solutions of Surfactants and for some Liquid Alkanes at 25 °C

surfactant/alkane	cmc, mol/L	τ_{uh}, *ns*
sodium decyl sulfate	0.008	0.2[59]
n-octyltrimethylammonium bromide	0.14	0.31[59]
n-decyltrimethylammonium bromide	0.06	0.22[59]
n-dodecyltrimethylammonium bromide	0.014	0.15[59]
n-tetradecyltrimethylammonium bromide	0.003	0.26[59]
n-hexadecyltrimethylammonium bromide	0.001	0.26[59]
1-palmitoyl-(63%), 1-stearoyl-(37%) glycero-3-phosphatidylcholine		0.13[60]
hexadecylsulfopropyl betaine	6×10^{-5}	0.24[60]
pentaethylene glycol monooctyl ether	0.009	0.23
pentaethylene glycol monododecyl ether	1×10^{-4}	0.23
n-decane	–	0.08[61]
n-dodecane	–	0.12[61]
n-tetradecane	–	0.19[38,61]
n-pentadecane	–	0.25[38]
n-hexadecane	–	0.29[38,61]

a chain conformational equilibrium to cause the ultrahigh-frequency relaxation process is thus an obvious idea. It is supported by the fact that in liquid alkanes a corresponding relaxation process exists (Table 10). The relaxation times for the alkanes are indeed somewhat smaller than for the micellar systems of identical chain length. This difference, however, is taken to reflect the different molecular order, since the hydrocarbon chains of micellar cores are fixed at the head groups. This fixing will probably enhance the microviscosity and promote cooperative effects within the cores. With the C_iE_j micelles parts of the poly(ethylene glycol) chains probably also participate in the structural isomerization.

Acknowledgment. We are indebted to Dr. A. Rupprecht and Dr. S. Z. Mirzaev for many discussions. Financial support by the Deutsche Forschungsgemeinschaft is gratefully acknowledged.

References and Notes

(1) Degiorgio, V., Corti, M., Eds. *Physics of Amphiphiles: Micelles, Vesicles and Microemulsions*; North-Holland: Amsterdam, 1985.
(2) Bellocq, A.-M. *Micelles, Membranes, Microemulsions and Monolayers*; Springer: Berlin, 1994.
(3) Frindi, M.; Michels, B.; Zana, R. *J. Phys. Chem.* **1992**, *96*, 6095.
(4) D'Arrigo, G.; Paparelli, A. *Phys. Rev. E* **1994**, *50*, 4817.
(5) Kato, S.; Harada, S.; Sahara, H. *J. Phys. Chem.* **1995**, *99*, 12570.
(6) Corti, M.; Degiorgio, V. *J. Chem. Phys.* **1981**, *85*, 1442.
(7) Hamano, K.; Yamashita, S.; Sengers, J. V. *Phys. Rev. Lett.* **1992**, *68*, 3579.
(8) Telgmann, T.; Kaatze, U. *J. Phys. Chem. A* **2000**, *104*, 1085.
(9) Eggers, F.; Kaatze, U.; Richmann, K. H.; Telgmann, T. *Meas. Sci. Technol.* **1994**, *5*, 1131.
(10) Kaatze, U.; Wehrmann, B.; Pottel, R. *J. Phys. E: Sci. Instrum.* **1987**, *20*, 1025.
(11) Kaatze, U.; Kühnel, V.; Menzel, K.; Schwerdtfeger, S. *Meas. Sci. Technol.* **1993**, *4*, 1257.
(12) Gailus, T. Dissertation, Georg-August-University, Göttingen, 1996.
(13) Kaatze, U.; Lautscham, K.; Brai, M. *J. Phys. E: Sci. Instrum.* **1988**, *21*, 98.
(14) Kaatze, U.; Kühnel, V.; Weiss, G. *Ultrasonics* **1996**, *34*, 51.
(15) Pakusch, A. Dissertation, Georg-August-University, Göttingen, 1983.
(16) Zielesny, A.; Belkoura, L.; Woermann, D. *Ber. Bunsen-Ges. Phys. Chem.* **1994**, *98*, 579.
(17) Binana-Limbelé, W.; Van Os, N. M.; Rupert, L. A. M.; Zana, R. *J. Colloid Interface Sci.* **1991**, *144*, 458.
(18) Schubert, K.-V.; Strey, R.; Kahlweit, M. *J. Colloid Interface Sci.* **1991**, *141*, 21.
(19) Corti, M.; Minero, C.; Degiorgio, V. *J. Phys. Chem.* **1984**, *88*, 309.
(20) Menzel, K.; Rupprecht, A.; Kaatze, U. *Acoust. Soc. Am.* **1998**, *104*, 2741.
(21) Bhattacharjee, J. K.; Ferrell, R. A. *Phys. Rev. A* **1981**, *24*, 1643.
(22) Ferrell, R. A.; Bhattacharjee, J. K. *Phys. Rev. A* **1985**, *31*, 1788.
(23) Telgmann, T.; Kaatze, U. *J. Phys. Chem. B* **1997**, *101*, 7758.
(24) Telgmann, T., Kaatze, U. *J. Phys. Chem. B* **1997**, *101*, 7766.
(25) Marquardt, D. W. *J. Soc. Indust. Appl. Math.* **1963**, *2*, 2.
(26) Press, W. H.; Tenkolsky, S. A.; Vetterling, W. T.; Flannery, B. P. *Numerical Recipes in C*; Cambridge University Press: Cambridge, 1992.
(27) Teubner, M. *J. Phys. Chem.* **1979**, *83*, 2917.
(28) Kahlweit, M.; Teubner, M. *Adv. Colloid Interface Sci.* **1980**, *13*, 1.
(29) Aniansson, E. A. G.; Wall, S. N. *J. Phys. Chem.* **1974**, *78*, 1024.
(30) Aniansson, E. A. G. *Prog. Colloid Polym. Sci.* **1985**, *70*, 2.
(31) Herzfeld, K. F.; Litovitz, T. A. *Absorption and Dispersion of Ultrasonic Waves*; Academic Press: New York, 1959.
(32) Matheson, A. J. *Molecular Acoustics*; Wiley-Interscience: London, 1971.
(33) Madigosky, W. M.; Warfield, R. W. *J. Chem. Phys.* **1983**, *78*, 1912.
(34) Madigosky, W. M.; Warfield, R. W. *Acustica* **1984**, *55*, 123.
(35) Kell, G. S. In *Water, a Comprehensive Treatise*; Franks, F., Ed.; Plenum: New York, 1972; Vol. 1, p 363.
(36) Telgmann, T. Dissertation, Georg-August-University, Göttingen, 1997.
(37) Zielesny, A.; Limberg, S.; Woermann, D. *Ber. Bunsen-Ges. Phys. Chem.* **1994**, *98*, 195.
(38) Behrends, R. Dissertation, Georg-August-University, Göttingen, 1999.
(39) D'Arrigo, G.; Briganti, G. *Phys. Rev. E* **1998**, *58*, 713.
(40) Hagen, R. Diploma-Thesis, Georg-August-University, Göttingen, 1998.
(41) Onuki, A. *Phys. Rev. E* **1997**, *57*, 403.
(42) Onuki, A. *J. Phys. Soc. Jpn* **1997**, *66*, 511.
(43) Folk, R.; Moser, G. *Phys. Rev. E* **1997**, *57*, 705.
(44) Folk, R.; Moser, G. *Phys. Rev. E* **1998**, *58*, 6246.
(45) Folk, R.; Moser, G. *Int. J. Thermophys.* **1998**, *19*, 1003.
(46) Fast, S. J.; Yun, S. S. *J. Acoust. Soc. Am.* **1988**, *83*, 1384.
(47) Bervillier, C.; Godrèche *Phys. Rev. B* **1980**, *21*, 5427.
(48) Würz, U.; Grubic, M.; Woermann, D. *Ber. Bunsen-Ges. Phys. Chem.* **1992**, *96*, 1460.
(49) Menzel, K. Dissertation, Georg-August-University, Göttingen, 1993.
(50) Belkoura, L.; Harnisch, F. P.; Kölchens, S.; Müller-Kirschbaum, T.; Woermann, D. *Ber. Bunsen-Ges. Phys. Chem.* **1987**, *91*, 1036.
(51) Sorensen, C. M.; Ackerson, B. J.; Mockler, R. C.; O'Sullivan, W. J. *Phys. Rev. A* **1976**, *13*, 1593.
(52) Sorensen, C. M.; Mockler, R. C.; O'Sullivan, W. J. *Phys. Lett. A* **1977**, *64*, 301.
(53) Martin, J. E.; Ackerson, B. J. *Phys. Rev. A* **1985**, *31*, 1180.
(54) Dueros, E.; Haonache, S.; Rouch, J.; Hamano, K.; Fukuhara, K.; Tartaglia, P. *Phys. Rev. E* **1994**, *50*, 1291.
(55) Hamano, K.; Ducros, E.; Louisor, E.; Rouch, J.; Tartaglia, P. *Physica A* **1996**, *231*, 144.
(56) Kawasaki, K. *Ann. Phys.* **1970**, *61*, 1.
(57) Kaatze, U. *Radiat. Phys. Chem.* **1995**, *45*, 549.
(58) Kaatze, U. *J. Solution Chem.* **1997**, *26*, 1049.
(59) Kaatze, U.; Lautscham, K.; Berger, W. *Z. Phys. Chem. NF* **1988**, *159*, 161.
(60) Kaatze, U.; Berger, W.; Lautscham, K. *Ber. Bunsen-Ges. Phys. Chem.* **1988**, *92*, 872.
(61) Kaatze, U.; Lautscham, K.; Berger, W. *Chem. Phys. Lett.* **1988**, *144*, 273.